
# SHocks: structure, AcceleRation, dissiPation

## Work Package 2
## Structure of heliospheric shocks

## Deliverable D2.2
## Technical report on the moderately supercritical shock front structure

Michael Gedalin [1], Ephim Golbraikh [1], Christopher T. Russell [2], Andrew P. Dimmock [3], Natalia Ganushkina [4], Max van de Kamp [4]

[1]Department of Physics, Ben Gurion University of the Negev, Beer-Sheva, Israel
[2]Department of Earth, Planetary, and Space Sciences, University of California, Los Angeles, California, USA
[3]Swedish Institute of Space Physics, Uppsala, Sweden
[4]Finnish Meteorological Institute, Helsinki, Finland 10/03/2022

This project has received funding from the European Union's Horizon 2020 research and innovation programme under grant agreement No 101004131

**Document Change Record**

| Issue | Date | Author | Details |
|---|---|---|---|
| 1.0 | 10.03.22 | M. Gedalin | send to the SHARP team for comments |
| 1.1 | 17.03.22 | M. Gedalin | final version |

# Table of Contents

# 1 Summary

Moderately supercritical shocks, with the Alfvénic Mach number of $\lesssim 5$, are expected to differ from low-Mach number of shocks in a number of ways: ion reflection causes appearance of the foot, the overshoot is more pronounced, the downstream magnetic oscillations may have a more complex pattern, and deviations from planarity and stationarity gradually become stronger. Some features of subcritical shocks, like a whistler precursor, may be present in moderately supercritical shocks too. As long as the nonplanarity (rippling) and time dependence remain weak, the theoretical predictions regarding the scales of the shock and the relation to the shock angle and the Mach number may be expected to remain approximately valid, as for low-Mach number subcritical shocks. These predictions were successfully verified versus observations for a supercritical Mercury (MESSENGER) shock and a terrestrial (MMS) shock (Gedalin et al., 2022a). The verification was partially based on the revision of the foot width of moderately supercritical shocks (Balikhin and Gedalin, 2022). In the earlier study (Gedalin, 2021) the overshoot strength was related to the cross-shock potential and ion distribution behind the ramp. A step towards development of a model of non-planar non-stationary shocks was done (Task 2.3 completed): an analytic model of the fields within a time-dependent rippled shock ramp was proposed and implications for the fields pattern upstream and downstream and for non-gyrotropic ion distributions downstream have been studied (Gedalin and Ganushkina, 2022b).

# 2 Introduction

The study is the direct continuation and generalisarion of the preceding study of the structure of subcritical shocks. Subcritical low-Mach number shocks are expected to have a monotonically increasing magnetic field profile of the ramp. Some of them have also an upstream coherent whistler wavetrain and a barely noticed overshoot. At larger Mach numbers in supercritical shocks a foot, an overshoot, and downstream magnetic oscillations develop (Farris et al., 1993; Bale et al., 2005), and gradually the shock front becomes rippled and/or time-dependent (Moullard et al., 2006; Burgess and Scholer, 2007; Lobzin et al., 2008; Yang et al., 2012; Ofman and Gedalin, 2013; Johlander et al., 2016; Gingell et al., 2017; Johlander et al., 2018; Hanson et al., 2019; Gedalin, 2019b; Madanian et al., 2021). Note that the Mach numbers of the shocks under study are still well below the range of expected reformation, so that time-dependence may be related directly to the ripples propagating along the shock front (Moullard et al., 2006; Ofman and Gedalin, 2013; Johlander et al., 2016; Omidi et al., 2021). Determination of the major shock scales and the Mach number from observations remains one of the central problem of the shock physics, essential for comparison with the theory. With the increase of the Mach number deviations from planarity and time-dependence make determination of the shock normal more difficult and one has to be careful to distinguish between the local and global normals (Ofman and Gedalin, 2013; Hanson et al., 2020). Nevertheless, for moderate Alfvénic Mach number of $M \lesssim 5$ we may still expect that the theoretical estimates of the whistler precursor wavelength (Krasnoselskikh et al., 2013) and the relation of the noncoplanar component of the magnetic field to the slope of the main magnetic field inside

the ramp (Jones and Ellison, 1987; Gosling et al., 1988; Gedalin, 1996; Newbury et al., 1997) should be approximately valid (Gedalin et al., 2022a). The widely used foot width estimate (Gosling and Thomsen, 1985) should have been revised since the assumption used there that the bulk ion flow is specularly reflected is unphysical. The distance between two successive maxima of downstream oscillations is estimated from the gyration of the downstream ion distributions (Gedalin et al., 2015; Gedalin, 2015, 2019a) and depends on the contribution of reflected ions. The Mercury (MESSENGER) and Earth (MMS) moderately supercritical shocks were used in this study to compare theory with observations and make an assessment of our understanding of the magnetic field profile of these shocks. The task required theoretical-numerical analysis of ion reflection in such shocks and re-estimate of the width of the foot produced by these ions (Balikhin and Gedalin, 2022).

The study, although important by itself, can be considered as a major intermediate stage in the task of proceeding from understanding low-Mach number shocks toward understanding high-Mach number non-planar non-stationary shocks. As a first step, we incorporated weak time-dependent rippling in the model of a shock front and analyzed the implications of such rippling on the pattern of the fields in the upstream and downstream regions adjacent to the ramp.

# 3 Detailed account or results

## 3.1 Comparison of existing theory with observations

Figure 1 shows a MESSENGER observed moderately supercritical shock and an MMS observed moderately supercritical shock. For both shocks the theoretical estimates of the noncoplanar magnetic field, foot width, the distance between the overshoot maximum and the undershoot minimum or the distance between two successive maxima are used to estimate the basic scales and the shock Mach number. For the MESSENGER shock the Mach number was derived by comparing the scales obtained by two methods. For the MMS shock the method was further verified via the standard approach with the particle data taken into account. The results are published in Gedalin et al. (2022a).

## 3.2 Foot width revisited

The widely used expression for the foot width (Gosling and Thomsen, 1985) is based on the assumption of specular reflection of the ions which enter the shock with the velocity equal to the velocity of the upstream flow in the normal incidence frame (NIF). This assumption cannot be valid, and the estimates of the shock-spacecraft closing speed from the above mentioned expression may be misleading. We have shown that ion reflection is significantly non-specular and occurs in the tail of the incident distribution and not in the core. Accordingly, the upstream turning distances of reflected ions depend on the cross-shock potential, as shown in Figure 2, and on the ratio $v_T/V_u$, where $v_T$ is the upstream thermal speed and $V_u$ is the NIF upstream flow speed. The actual foot width appears about half of the currently used value. The results are published in Balikhin and Gedalin (2022).

### 3.3 Overshoot relation to ion motion

The shock width is substantially smaller than the ion convective gyroradius. The ion motion in the ramp and up to the maximum of the overshoot is governed mainly by the cross-shock electric field. This motion can be analyzed within hydrodynamics of demagnetized ions (as opposed to magnetized electrons) or single particle motion with subsequent application of the Liouville mapping. If the contribution of the reflected ions is small, the main effect is the deceleration of the directly transmitted ions. The momentum lost by the ions is absorbed by the increasing magnetic field. The conservation law predicts a simple relation between the maximum magnetic field $B_m$, the Mach number $M$, and the cross-ramp potential $s_r = 2e\varphi/m_p V_u^2$:

$$\left(\frac{B_m}{B_u}\right)^2 = 2M^2(1-\sqrt{1-s_r})+1 \tag{1}$$

This is a crude but useful relation which allowed also to propose a proxy for the Mach number. These results were published in Gedalin (2021).

### 3.4 Weak non-planarity and non-stationarity

A model of a weakly non-planar weakly non-stationary shock is proposed as a weak rippling of the shock ramp propagating along the shock front. A rather general model of the localized rippling is used to derive the deviations of the fields from the stationary planar shape inside the ramp. It is shown that certain parameters of the rippling can be estimated by comparing various components of the magnetic and electric field inside the ramp (see, for example, Figure 3 for visualization) It is concluded that the ramp should generate waves which are diverging from the ramp into the upstream and downstream regions. A relation of the wavelength of the corresponding upstream whistler to the rippling parameters is established. Two-fluid approach has been analyzed separately in the upstream region, inside the ramp, and in the downstream region. The major differences are for ions since for electrons the massless approximation is good enough for the spatial and temporal scales of interest. The ion fluid description in the upstream region is not affected much by the rippling induced modifications of the fields. The ion hydrodynamics inside the ramp largely follows the same demagnetized pattern as was in the stationary planar case, while the points of entry to and exit from the ramp depend on the position along the shock front and time. Corrections to the ion motion are proportional to the rippling amplitude, that is, the maximum shift of the central part of the ramp along the shock normal, relative to the stationary planar position. The downstream ion distributions should exhibit the same pattern as the rippling, with enhanced gyrophase mixing and collisionless relaxation further downstream. The corrections to the conservation laws are derived. These corrections are also proportional to the rippling amplitude, which means that flux and total pressure still remain approximately constant along the shock normal. The work is theoretical, yet the results and conclusions are aimed on use with observations and numerical simulations. The study is summarized in the paper "Implications of weak rippling of the shock ramp on the pattern of the electromagnetic field and ion distributions" (M. Gedalin and N. Ganushkina), which is submitted for publication (Gedalin and Ganushkina, 2022b).

# 4 Conclusions

To summarize, we have achieved the following:

- It has been shown that the shock structure of a moderately supercritical shock is stationary and planar within a good approximation. Our theoretical understanding of the shock structure, including the scales of the main features, is rather good.
- An improved estimate of the foot width has been obtained. The foot width estimate is one of the most often used tools in the determination of the shock speed in the spacecraft frame and subsequent conversion of the temporal measurements into spatial characteristics.
- A relation has been established between the overshoot maximum and the ion motion in the shock field.
- A theoretical model of a weakly rippled shock has been proposed and implications for observations and numerical simulations have been analyzed.

The achievements complete the tasks 2.2 and 2.3. It is worth noticing that, although the research is split in well-defined tasks, the physical problems described in different tasks and inter-related. Therefore, while working on specific task contribution to other tasks is often achieved. The results, obtained in the studies reported previously in the deliverable D2.1 and here in the deliverable D2.2, contribute also to the tasks 2.5, 2.6, and 3.1.

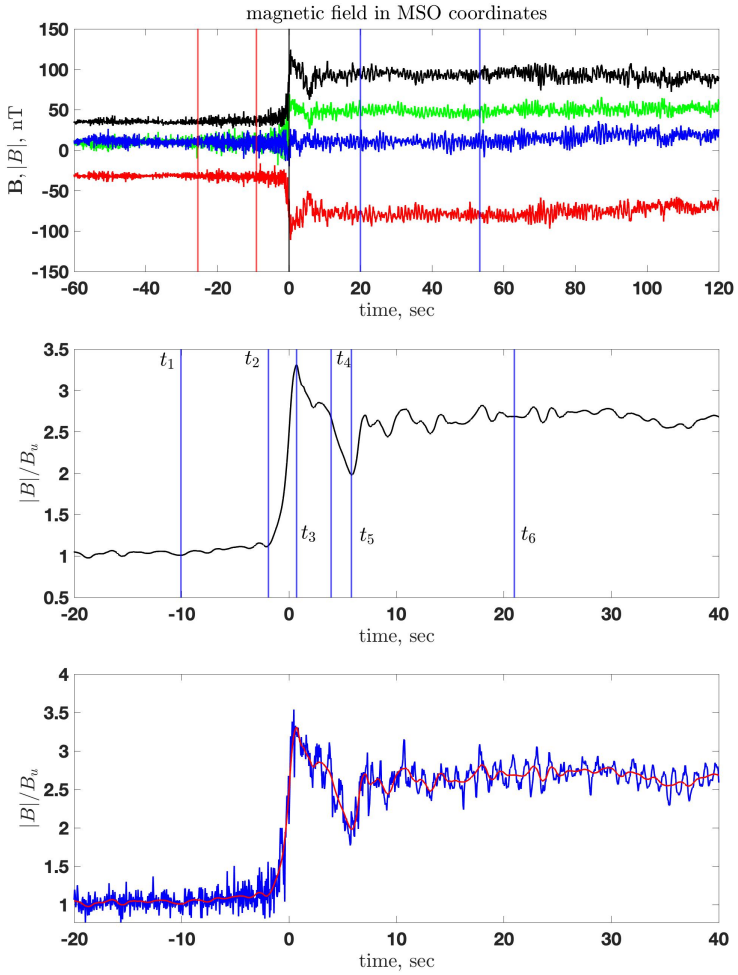


Figure 1: Top: a MESSENGER measured moderately supercritical shock. The magnetic field in MSO coordinates: $B_x$ (green), $B_y$ (red), $B_z$ (blue), and $|\mathbf{B}|$ (black), for the shock crossing 2013/047/06:57:00. The red vertical lines mark the upstream region used for the calculation the normal from magnetic coplanarity, the blue vertical lines mark the downstream region. Time is measured in sec from the shock crossing (marked by the black vertical line). Middle: the denoised $B$ and the meaningful points, from left to right: the beginning of the foot ($t_1$), the end of the foot and the beginning of the ramp ($t_2$), the overshoot maximum ($t_3$), the point where the magnetic field decreases to the value nearly equal to the downstream magnetic field magnitude ($t_4$), the minimum of the undershoot ($t_5$), the point where the mean magnetic field essentially levels off ($t_6$). Bottom: a MMS measured moderately supercritical shock. The black line shows the normalized magnetic field magnitude. The red line show the denoised magnetic field. The vertical blue lines show the beginning and the end of the foot.

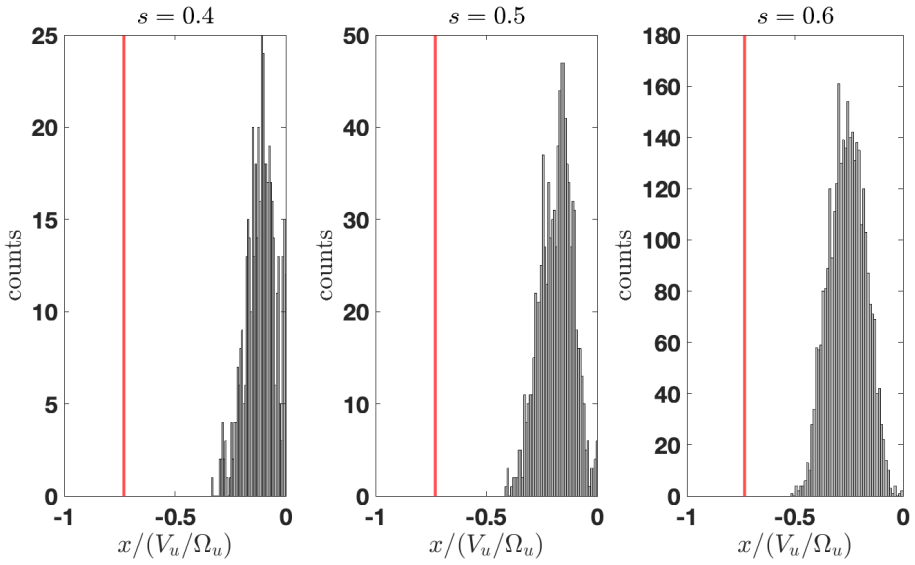


Figure 2: Histograms of the turning distances of the reflected ions in the foot for $\theta_{Bn} = 70°$, $\beta = 0.3$, and three values of the cross-shock potential $s = 2e\varphi/m_p V_u^2 = 0.4, 0.5, 0.6$. The red line marks the position of the upstream edge of the foot according to Gosling and Thomsen (1985).

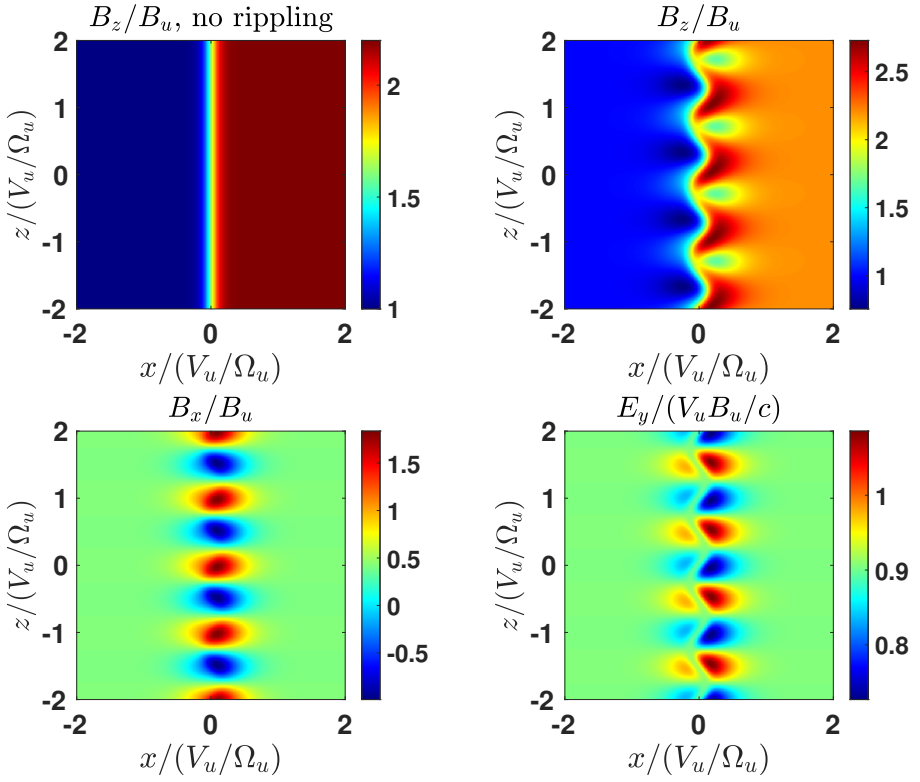


Figure 3: Top left: $B_z$ for a stationary planar shock. Top right: $B_z$ for a rippled shock. Bottom left: $B_x$ for a rippled shock. Bottom right: $E_y$ for a rippled shock. Parameters are given in text.

# 5 References

S D Bale, M A Balikhin, T S Horbury, V V Krasnoselskikh, H Kucharek, E Möbius, S N Walker, A Balogh, D Burgess, B Lembège, E A Lucek, M Scholer, S J Schwartz7 10, and M F Thomsen. Quasi-perpendicular Shock Structure and Processes. *Sp. Sci. Rev.*, 118, 161m 2005. doi: 10.1007/s11214-005-3827-0.

M. Balikhin and M. Gedalin. Collisionless Shocks in the Heliosphere: Foot Width Revisited. *Astrophys. J.*, 925, 90, 2022. doi: 10.3847/1538-4357/ac3bb3.

D Burgess and M Scholer. Shock front instability associated with reflected ions at the perpendicular shock. *Phys. Plasmas*, 14, 012108, 2007. doi: 10.1063/1.2435317.

M Farris, C Russell, and M Thomsen. Magnetic structure of the low beta, quasi-perpendicular shock. *J. Geophys. Res.*, 98, 15285, 1993.

M Gedalin. Noncoplanar magnetic field in the collisionless shock front. *J. Geophys. Res.*, 101, 11153, 1996. doi: 10.1029/96JA00518.

M Gedalin. Collisionless relaxation of non-gyrotropic downstream ion distributions: dependence on shock parameters. *J. Plasma Phys.*, 81, 905810603, 2015. doi: 10.1017/S0022377815001154.

M Gedalin. Transmitted, reflected, quasi-reflected, and multiply reflected ions in low-Mach number shocks. *J. Geophys. Res*, 121, 10, 2016. doi: 10.1002/2016JA023395.

M Gedalin, Y Friedman, and M Balikhin. Collisionless relaxation of downstream ion distributions in low-Mach number shocks. *Phys. Plasmas*, 22, 072301, 2015. doi: 10.1063/1.4926452.

M. Gedalin. Kinematic Collisionless Relaxation of Ions in Supercritical Shocks. *Frontiers in Physics*, 7, 692, 2019a. doi: 10.3389/fphy.2019.00114.

M. Gedalin. How non-stationary are moderately supercritical shocks? *J. Plasma Phys.*, 85, 905850505, 2019b. doi: 10.1017/S0022377819000692.

M. Gedalin. Shock Heating of Directly Transmitted Ions. *Astrophys. J.*, 912, 82, 2021. doi: 10.3847/1538-4357/abf1e2.

M. Gedalin, E. Golbraikh, C. T. Russell, and A. P. Dimmock. Theory helps observations: Determination of the shock Mach number and scales from magnetic measurements, Frontiers of Physics, 2022a (in press).

M. Gedalin and N. Ganushkina. Implications of weak rippling of the shock ramp on the pattern of the electromagnetic field and ion distributions, J. Plasma Phys. (submitted).

I. Gingell, S. J. Schwartz, D. Burgess, A. Johlander, C. T. Russell, J. L. Burch, R. E. Ergun, S. Fuselier, D. J. Gershman, B. L. Giles, K. A. Goodrich, Y. V. Khotyaintsev, B. Lavraud, P. A. Lindqvist, R. J. Strangeway, K. Trattner, R. B. Torbert, H. Wei, and F. Wilder. MMS Observations and Hybrid Simulations of

Surface Ripples at a Marginally Quasi-Parallel Shock. *J. Geophys. Res*, 77, 736, 2017. doi: 10.1002/2017JA024538.

J T Gosling and M F Thomsen. Specularly reflected ions, shock foot thicknesses, and shock velocity determinations in space. *J. Geophys. Res*, 90, 9893, 1985. doi: 10.1029/JA090iA10p09893.

J. T. Gosling, D. Winske, and M. F. Thomsen. Noncoplanar magnetic fields at collisionless shocks: A test of a new approach. *J. Geophys. Res*, 93, 2735, 1988. ISSN 0148-0227. doi: 10.1029/JA093iA04p02735.

E L M Hanson, O V Agapitov, F S Mozer, V Krasnoselskikh, S D Bale, L Avanov, Y Khotyaintsev, and B Giles. Cross-Shock Potential in Rippled Versus Planar Quasi-Perpendicular Shocks Observed by MMS. *Geophys. Res. Lett.*, 46, 2381, 2019. doi: 10.1029/2018GL080240.

E L M Hanson, O V Agapitov, F S Mozer, V Krasnoselskikh, S D Bale, L Avanov, B L Giles, and R B Torbert. Terrestrial Bow Shock Parameters From MMS Measurements: Dependence on Upstream and Downstream Time Ranges. *J. Geophys. Res*, 125, 1, 2020. doi: 10.1029/2019JA027231.

A Johlander, S J Schwartz, A Vaivads, Yu V Khotyaintsev, I Gingell, I B Peng, S Markidis, P A Lindqvist, R E Ergun, G T Marklund, F Plaschke, W Magnes, R J Strangeway, C T Russell, H Wei, R B Torbert, W R Paterson, D J Gershman, J C Dorelli, L A Avanov, B Lavraud, Y Saito, B L Giles, C J Pollock, and J L Burch. Rippled Quasiperpendicular Shock Observed by the Magnetospheric Multiscale Spacecraft. *Phys. Rev. Lett.*, 117, 165101, 2016. doi: 10.1103/PhysRevLett.117.165101.

A. Johlander, A. Vaivads, Y V Khotyaintsev, I. Gingell, S. J Schwartz, B. L Giles, R. B Torbert, and C. T Russell. Shock ripples observed by the MMS spacecraft: Ion reflection and dispersive properties. *Plasma Phys. Contr. Fusion*, 60, 125006, 2018. doi: 10.1088/1361-6587/aae920.

F. C. Jones and D. C. Ellison. Noncoplanar magnetic fields, shock potentials, and ion deflection. *J. Geophys. Res*, 92, 11205, 1987. doi: 10.1029/JA092iA10p11205.

V Krasnoselskikh, M Balikhin, S N Walker, S Schwartz, D Sundkvist, V Lobzin, M Gedalin, S D Bale, F Mozer, J Soucek, Y Hobara, and H Comişel. The Dynamic Quasiperpendicular Shock: Cluster Discoveries. *Sp. Sci. Rev.*, 178, 535, 2013. doi: 10.1007/s11214-013-9972-y.

V V Lobzin, V V Krasnoselskikh, K Musatenko, and T Dudok de Wit. On nonstationarity and rippling of the quasiperpendicular zone of the Earth bow shock: Cluster observations. *Annales Geophysicae*, 26, 2899, 2008. doi: 10.5194/angeo-26-2899-2008.

H Madanian, M I Desai, S J Schwartz, L B Wilson, S A Fuselier, J L Burch, O Le Contel, D L Turner, K Ogasawara, A L Brosius, C T Russell, R E Ergun, N Ahmadi, D J Gershman, and P A Lindqvist. The Dynamics of a High Mach

Number Quasi-perpendicular Shock: MMS Observations. *Astrophys. J.*, 908, 40, 2021. doi: 10.3847/1538-4357/abcb88.

O Moullard, D Burgess, T S Horbury, and E A Lucek. Ripples observed on the surface of the Earth's quasi-perpendicular bow shock. *J. Geophys. Res*, 111, A09113, 2006. doi: 10.1029/2005JA011594.

J A Newbury, C T Russell, and M Gedalin. The determination of shock ramp width using the noncoplanar magnetic field component. *Geophys. Res. Lett.*, 24, 1975, 1997. doi: 10.1029/97GL01977.

L Ofman and M Gedalin. Rippled quasi-perpendicular collisionless shocks: Local and global normals. *J. Geophys. Res*, 118, 5999, 2013. doi: 10.1002/2013JA018780.

N. Omidi, M. Desai, C. T. Russell, and G. G. Howes. High Mach Number Quasi-Perpendicular Shocks: Spatial Versus Temporal Structure. *J. Geophys. Res*, 126, e2021JA029, 2021. doi: 10.1029/2021JA029287.

Z W Yang, B Lembège, and Q M Lu. Impact of the rippling of a perpendicular shock front on ion dynamics. *J. Geophys. Res*, 117, A07222, 2012. doi: 10.1029/2011JA017211.